
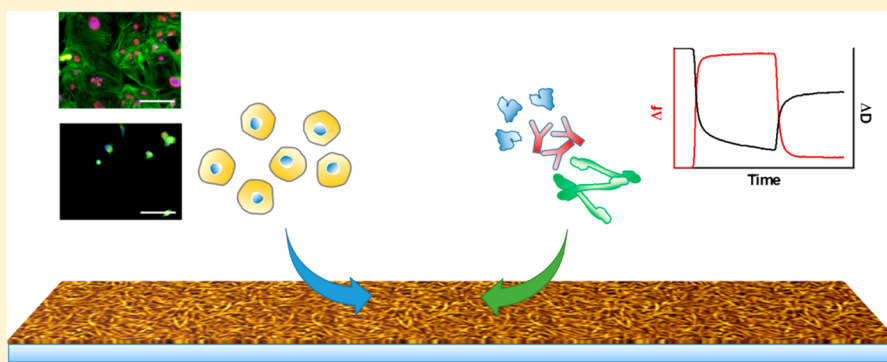


Cell and Protein Fouling Properties of Polymeric Mixtures Containing Supramolecular Poly(ethylene glycol) Additives

A. C. H. Pape,^{†,‡} Bastiaan D. Ippel,^{†,§} and Patricia Y. W. Dankers^{*,†,‡,§} 

[†]Institute for Complex Molecular Systems, [‡]Laboratory for Chemical Biology, and [§]Laboratory for Cell and Tissue Engineering, Eindhoven University of Technology, P.O. Box 513, 5600 MB Eindhoven, The Netherlands

Supporting Information



ABSTRACT: Fouling properties of new biomaterials are important for the performance of a material in a biological environment. Here, a set of three supramolecular polymeric additives consisting of ureidopyrimidinone (UPy)-functionalized poly(ethylene glycol) (UPyPEG) were formulated with UPy-modified polycaprolactone into thin supramolecular material films. The antifouling properties of these material films were determined by investigation of the relation of cell adhesion and protein adsorption on these materials films. The presence of the UPyPEG additives at the surface of the films was evident by an increased hydrophilicity. Adhesion of human epithelial and endothelial cells was strongly reduced for two of the UPyPEG-containing films. Analysis of adsorption of the first three proteins from the Vroman series, albumin, γ -globulin, and fibrinogen, using quartz crystal microbalance with dissipation in combination with viscoelastic modeling, revealed that the surfaces containing the UPyPEG additives had a limited effect on adsorption of these proteins. Despite a limited reduction of protein adsorption, UPyPEG-containing mixtures were non-cell-adhesive, which shows that non-cell-adhesive properties of supramolecular polymer surfaces are not always directly correlated to protein adsorption.

■ INTRODUCTION

Control of the fouling properties of biomaterials, e.g., protein adsorption and cell adhesion, is essential for ultimate functioning of these materials as implants and prostheses. Surface coating of implants using antifouling compounds is often applied. Functional antifouling properties are most frequently added through physisorption or chemical tethering of nonfouling moieties. Covalently attached layers are more durable than physisorbed adlayers, but making stable coatings on more complex surfaces as efficient in reducing biofouling as self-assembling monolayers (SAMs) on gold remains a challenge.¹

Initial investigation on properties of antifouling SAMs revealed that moieties that resist the adsorption of proteins and cells typically are hydrophilic, include hydrogen-bond acceptors, but do not include hydrogen-bond donors, and have an overall neutral charge.^{2,3} Since then, hydrophilic poly(ethylene glycol) (PEG)-based materials have been widely used to develop antifouling surfaces using varying surface preparation techniques.⁴ Similar to hydrophilic polysaccharide

containing materials and coatings based on zwitterionic molecules, the antifouling properties of PEG-based materials have been attributed to the presence of an hydration layer near the surface, which acts as a barrier.⁵

To design antifouling materials, ethylene glycol-based materials have been used in varying designs.⁵ Recently, the functionalization of substrates with polymer brushes has proven to increase surface coverage and thereby increase effectiveness of the applied coating.^{1,6} Brush-like coatings based on PEG, often in the form of a poly[oligo(ethylene glycol) methyl methacrylate] (polyOEGMa), have for instance been successfully applied via surface-initiated atom transfer radical polymerization (SI-ATRP) on 2D substrates^{7,8} and on electrospun fibers.^{9,10}

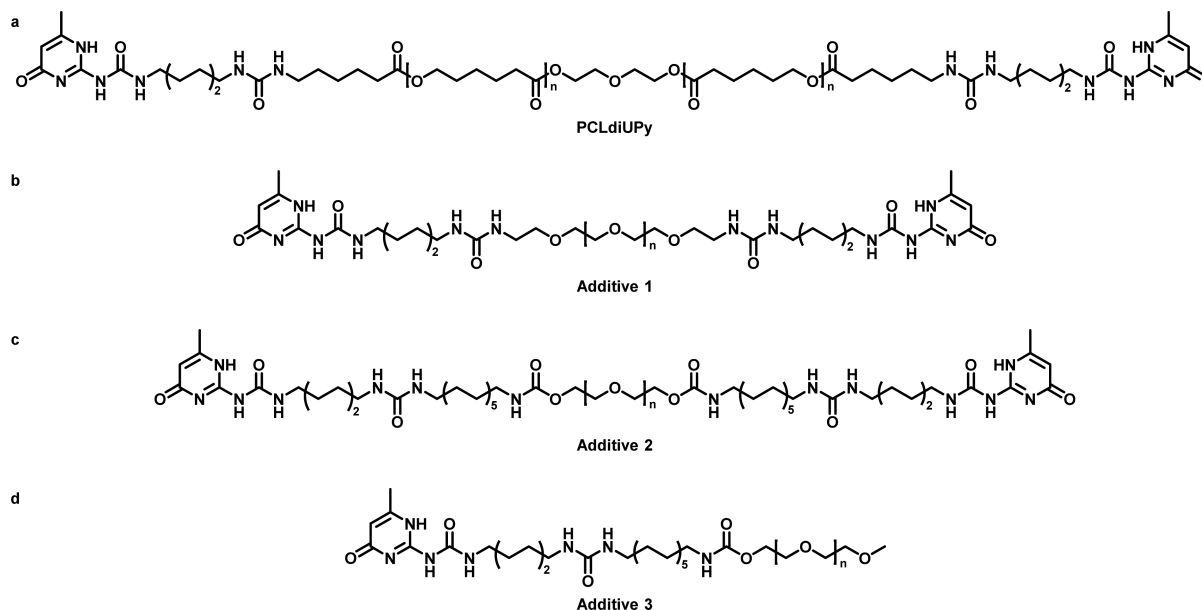
Cell adhesion is presumed to be preceded by nonspecific protein adsorption, which agrees to the fact that PEG-

Received: February 10, 2017

Revised: March 22, 2017

Published: March 31, 2017

Scheme 1. Chemical Structures of the Molecules Used in This Study: (a) UPy-Modified Polycaprolactone ($M_{n,PCL} = 2$ kDa); (b) Bifunctional UPy Poly(ethylene glycol) ($M_{n,PEG} = 2$ kDa); (c) Bifunctional PEG_{10K}diUPy ($M_{n,PEG} = 10$ kDa); (d) Monofunctional UPyPEG ($M_{n,PEG} = 5$ kDa)



functionalized materials often show a decrease in protein adsorption when a reduction in cell adhesion is also observed.^{2,6,9,11,12} The first proteins to adsorb upon contact with the biomaterial are high mobility proteins, such as albumin. Subsequently, displacement by less abundant proteins with higher affinities occurs, starting with globulin and fibrinogen, and ending with high molecular weight kininogen. This process is called the Vroman effect.¹³

To quantitatively measure the adsorption of proteins on biomaterial surfaces *in vitro*, several techniques have been used, such as fluorescence microscopy, ellipsometry, surface plasmon resonance (SPR), and quartz crystal microbalance with dissipation (QCM-D).^{1,14} QCM-D offers label-free frequency and real-time monitoring of the hydrated mass adsorption using the change in resonance frequency and dissipation energy of a piezoelectric quartz crystal with a resolution of 1 ng/cm².¹⁵ Recently, protein adsorption has been investigated on spin-coated layers of different thermoplastic polyurethanes¹⁶ and on varying antifouling coatings containing chondroitin sulfate, PEG, carboxymethylated dextran, or zwitterions.^{17–20}

Our approach to new biomaterials applies an alternative strategy. Using noncovalent supramolecular interactions, based on the self-complementary 2-ureido-4[1H]-pyrimidinone (UPy) moiety,²¹ we were able to develop modular biomaterials with UPy-modified polycaprolactone (PCLdiUPy) (Scheme 1) as the structural base material.^{22–24} More recently, this system has been further expanded by the incorporation of PEG_{2K}diUPy (additive 1, Scheme 1) to prevent cell adhesion.²⁵ Previously, we have shown that the addition of PEG_{2K}diUPy reduces the hydrophobicity of the surface, leads to decreased cell adhesion on electrospun meshes *in vitro*,²⁵ and reduces cell infiltration *in vivo* in a chain-extended UPy-modified PCL material.²⁶

Here, our supramolecular toolbox is extended with bifunctional PEG_{10K}diUPy (additive 2, Scheme 1) and monofunctional MeOPEG_{5K}UPy (additive 3, Scheme 1), previously used as hydrogelators.²⁷ These additives are of interest because they contain larger PEG chains and hence could lead to more hydrophilic surfaces and thus less cell adhesion. Furthermore,

both compounds contain an extra aliphatic dodecyl spacer between the UPy and the PEG, which can shield the urea groups from interactions with water of the PEG and can lead to enhanced anchoring in the PCLdiUPy base material. The MeOPEG_{5K}UPy mimics half of the PEG_{10K}diUPy and therefore allows investigation of the effect of the number of anchoring points. With our previous results, and the presumption that cell adhesion is preceded by nonspecific protein adsorption, investigation of protein adsorption on our materials provides more insight into the non-cell-adhesive properties of the PEG-containing materials.

The surface morphology of the spin-coated supramolecular polymer films was studied using atomic force microscopy (AFM) and water contact angle (WCA) measurements. The adhesion of epithelial and endothelial cells on the polymer film was investigated, and the adsorption of the first three proteins of the Vroman series¹³ (albumin, globulin, and fibrinogen) was quantified using QCM-D.

EXPERIMENTAL SECTION

Materials. PCLdiUPy and PEG_{10K}diUPy were synthesized by SyMO-Chem BV (Eindhoven, The Netherlands). The syntheses of PEG_{2K}diUPy²⁵ and MeOPEG_{5K}UPy²⁷ were described previously. PBS tablets, 1,1,1,3,3,3-hexafluoroisopropanol (HFIP), EDTA, non-idet NP-40, gelatin from porcine skin, bovine serum albumin (BSA), fibrinogen from bovine plasma, γ -globulins from bovine blood, mowiol 4-88, anti-human vinculin mouse IgG1 antibody (V9131), ATTO 488 conjugated phalloidin, and 4',6-diamidino-2-phenylindole (DAPI) were purchased from Sigma-Aldrich (Zwijndrecht, The Netherlands). EGM-2 Bulletkit, penicillin/streptomycin, and trypsin/EDTA were purchased from Lonza (Breda, Netherlands). Alexa 555 conjugated goat anti-mouse IgG1 was purchased from Molecular Probes. Tris, NaCl, and Triton X-100 were purchased from Merck Millipore, fetal bovine serum (FBS) from Greiner Bio, and Dulbecco's Modified Eagle Medium (#41966) from Gibco Life Sciences. BSA, fibrinogen, and γ -globulins were obtained as powders and used without further purification.

Preparation of Polymer Solutions. Solutions of all polymers were prepared at a concentration of 20 mg/mL in HFIP. For the

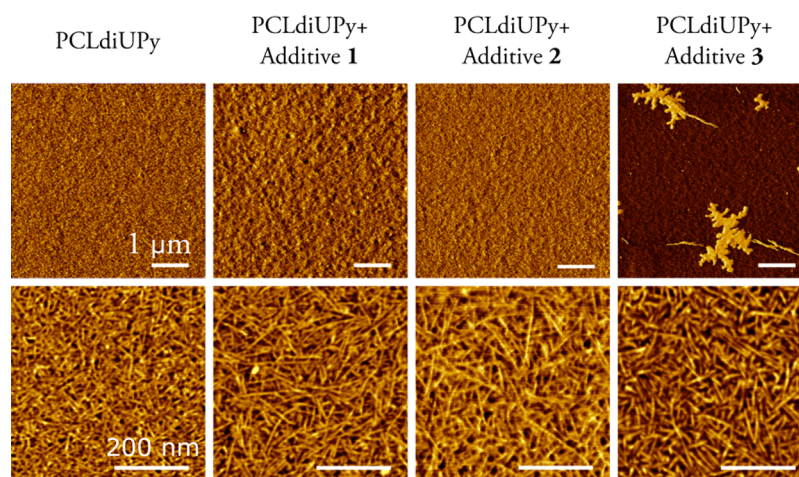


Figure 1. AFM phase micrographs of spin-coated films of PCLdiUPy with 5 wt % of the UPyPEG additives on glass.

mixtures, 5 vol % of the additive polymer solution was added to 95 vol % solution of PCLdiUPy. This results in 5:95 wt % additive:PCLdiUPy mixtures, corresponding to 5, 1.24, and 2.45 mol % mixtures for additive 1, 2, and 3, respectively (Table S7; calculation is provided in the Supporting Information).

Preparation of Spin-Coated Surfaces. Samples were prepared by spin-coating 100 μL of a 20 mg/mL solution of the polymers in HFIP at 5000 rpm for 30 s on either glass coverslips with a diameter of 15 mm (for AFM) or 13 mm (for cell culture) or on the gold-coated sensor (for QCM-D). The samples were left to dry for 1 h at room temperature before continuing the experiments.

Atomic Force Microscopy. AFM images were recorded at room temperature using a Digital Instrument Multimode Nanoscope IV operating in the tapping regime mode using silicon cantilever tips (PPP-NCH-50, 204–497 kHz, 10–130 N/m). Surface roughness has been measured using Gwyddion software (version 2.34). The root-mean-square (RMS) for an area of 100 μm^2 was used to compare the different materials.

Water Contact Angle Measurements. Water contact angles were measured at room temperature on an OCA30 (DataPhysics). Water droplets (5 μL) were applied on the polymer films on glass, and the angle at the polymer–air–water interface was determined after 5 s using an automatic fitting routine (SCA20 software). The mean and the standard deviation of three samples are reported.

Cell Culture. Human umbilical vein endothelial cells (HUVEC, Lonza) were cultured in EGM-bulletkit medium (endothelial basal medium supplemented with 2% FBS and growth factors, including VEGF) supplemented with 1% penicillin/streptomycin and expanded in T-75 culture flasks that were coated with a 0.1% gelatin solution for 15 min at 37 $^{\circ}\text{C}$. Proximal epithelial cells from a human kidney (HK-2, ATCC) were cultured in DMEM, supplemented with 10% FBS and 1% penicillin/streptomycin, and expanded in T-75 culture flasks. Cells were subcultured at a 80–90% confluency by washing with PBS and incubating in 2 mL of trypsin/EDTA for 1–2 min (HUVEC) and 3–5 min (HK-2) at 37 $^{\circ}\text{C}$ and diluted in 8 mL of culture medium before centrifugation for 5 min at 180g. Cells were resuspended and counted using a NucleoCounter (NC-100, Chemometec Copenhagen, Denmark) and diluted to 8–104 cells/mL culture medium and reseeded at 106 cells per T-75 flask. Culture medium was refreshed every 2–3 days. HUVECs were used for experiments up to P5 and HK-2 cells up to P16.

Cell Seeding. Glass coverslips with a diameter of 13 mm (#0, VWR), either covered with spin-coated polymer, coated with gelatin, or bare, were placed in Minusheet tissue carriers with 13 mm o.d. (Minucells and Minutissue-Vertriebs GmbH) to prevent films from detaching during culture and were then sterilized under UV for 1 h. Next, the secured coverslips were placed in 24 wells culture plates, and 250 μL culture medium was pipetted under the coverslip. Cells were harvested as in subculture and resuspended in culture medium and

diluted to 2.6×10^5 cells/mL. 62 μL of cell suspension was pipetted onto the exposed surface of the coverslips, and cells were left to adhere for 1.5 h at 37 $^{\circ}\text{C}$ and 5% CO_2 , before adding 500 μL of culture medium on top of the cells. Cells were cultured for 1 day at 37 $^{\circ}\text{C}$ and 5% CO_2 .

Immunofluorescent Staining. Cells grown on coverslips were fixed and permeabilized simultaneously by incubation in 3.7% formaldehyde and 0.5% Triton X-100 in PBS for 15 min at room temperature. Samples were then washed with PBS twice and subsequently blocked in 2% BSA at least overnight at 4 $^{\circ}\text{C}$. Next, slips were washed in NET-gel (50 mM Tris, 150 mM NaCl, 5 mM EDTA, 0.05% NP-40 and 0.25% gelatin), prior to overnight incubation with primary mouse IgG1 anti-human vinculin antibody 1:250 in 80% NET-gel and 1% BSA in PBS at 4 $^{\circ}\text{C}$. Samples were then washed in NET-gel three times and subsequently incubated for 1.5 h at room temperature with 1:250 goat anti-mouse IgG1 Alexa 555 conjugated secondary antibody and 1:500 ATTO 488 conjugated phalloidin in NET-gel, followed by a double 5 min wash in NET-gel and a nuclear counterstain with 0.1 $\mu\text{g}/\text{mL}$ DAPI in PBS. After three washes in PBS, coverslips were mounted on microscopy slides with mowiol and stored in the dark at 4 $^{\circ}\text{C}$ until visualization with a Zeiss AxioVert 200 M microscope.

Quartz Crystal Microbalance with Dissipation Monitoring. QCM-D was performed on the Q₂-Sense E4 instrument (BiolinScientific AB) using gold-coated AT-cut quartz discs with a fundamental frequency of 4.95 MHz (QX3 301 Gold, BiolinScientific AB). Sensors were rinsed with piranha solution and subsequently heated for 10 min at 70 $^{\circ}\text{C}$ in a 5:1:1 mixture of ultrapure water, ammonia, and 30% hydrogen peroxide (base piranha). Sensors were rinsed with water, acetone, and isopropanol and dried with nitrogen. Clean crystals were mounted to record their fundamental frequency in air and subsequently removed for spin-coating. All experiments were performed at 37 $^{\circ}\text{C}$. After mounting the sensors with the spin-coated material, sensors were measured in air. Afterward, PBS was passed over the surface at 0.1 mL/min until the signal equilibrated. Subsequently, the protein solution was passed over the surface at 0.1 mL/min. Frequency and dissipation changes were recorded until both signal equilibration, and the sensors were rinsed with PBS. Each experiment was repeated 3-fold, and means and standard errors of the mean are reported.

After each experiment, the system was cleaned by rinsing with 50 mL of 2 wt % solution of Hellmanex III (Hellma) in ultrapure water, followed by rinsing with 100 mL of ultrapure water. Next, sensors were removed and the components were dried using nitrogen.

Viscoelastic Modeling of the Data. Shifts in frequency and dissipation for overtones 3, 5, 7, 9, and 11 were analyzed using the Voigt–Voinova model using the Qtools software (Q-sense). A protein density of 1250 kg/m^3 was used for all protein layers. As became evident from the measurements, the viscosity of the protein solutions

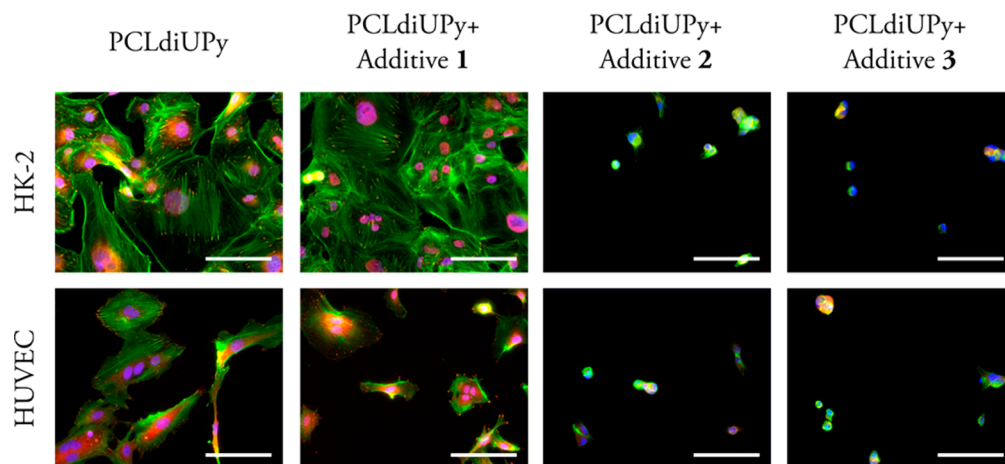


Figure 2. Fluorescence microscopy images of HK-2 cells and HUVECs cultured on spin-coated polymer films for 1 day, stained for f-actin (green), vinculin (red), and nuclei (blue). Scale bars represent 100 μm .

was higher than the viscosity of PBS and hence was accounted for in the model, together with one homogeneous viscoelastic layer. For PBS at 37 $^{\circ}\text{C}$, the measured viscosity in the QCM-D was 0.0071 Pa s, and a density of 1000 kg/m^3 was used. The model was optimized by decreasing χ^2 by optimizing the selection of overtones.

RESULTS AND DISCUSSION

Surface Morphology Polymer Films. The use of QCM-D to quantify protein adsorption requires a homogeneous and thin polymer film. Initial experiments showed that drop-casting leads to thick films in the micrometer range at higher concentrations or to inhomogeneous films caused by dewetting at lower concentrations. Therefore, spin-coating was selected as the technique to reproducibly prepare thin polymer films. The surface roughness of the polymer films prepared by spin-coating was assessed using AFM (Table S1). The addition of UPy-PEG did slightly increase the RMS roughness for spin-coated samples, but no large differences are observed. AFM phase images show a fibrous morphology on the nanometer length scale for pristine PCLdiUPy films, similar to nanofibers obtained previously in drop-cast samples, attributed to the highly directional self-assembly of the combined UPy and urea moieties.²³ When 5 wt % of additive 1 was added, a similar nanofibrillar morphology is observed (Figure 1). For the samples with additive 3, domains of PEG can be observed on the larger scale, which were also visible in the height images (Figure S1). Details of the microphase-separated regions show PCLdiUPy-like fibers in the darker regions while the lighter regions are hypothesized to represent the PEG phase. A homogeneous polymer film was obtained for mixtures with additive 2, with well-defined fibrillar morphology. We hypothesize that the speed of spin-coating inhibits both nanophase and microphase separation, leading to suboptimal fiber formation, but intimate mixing of the components.

WCA measurements were performed to assess surface hydrophilicity. For the pristine PCLdiUPy the water contact angle is $74.7 \pm 0.2^{\circ}$. A sharp decrease in contact angles is observed with the addition of UPyPEG, with contact angles of $59.8 \pm 1.3^{\circ}$ for PCLdiUPy with additive 1, $56.7 \pm 0.9^{\circ}$ with additive 2, and $44 \pm 14^{\circ}$ with additive 3. The presence of the hydrophilic components in the films prepared from the polymer mixtures is clearly reflected in the water contact angles.

Cell Adhesion on Polymer Mixtures. The adhesive behavior of cells on our materials with the different PEG-

containing additives was evaluated based on the staining of f-actin, an important part of the cytoskeleton, and vinculin, a focal adhesion protein involved in anchoring these microfilaments to the extracellular matrix.²⁸ On PCLdiUPy and the mixture with additive 1, HK-2 cells show a well-spread morphology and clear actin fibers, terminating in defined vinculin spots, indicating good adhesion (Figure 2, and single channel greyscale images in Figure S2). Less HUVECs adhered to PCLdiUPy and the mixture with additive 1 than HK-2 cells and show a decrease in cell spreading (Table S6). Moreover fewer vinculin spots are observed, indicating less firm adhesion to the material. Both HK-2 cells and HUVECs show a clear decrease in adhesion and spreading on the mixtures with additives 2 and 3 (Table S6). Cells show a rounded morphology and have a lack of actin fibers and vinculin spots. Previous studies show a significant decrease in cell adhesion materials functionalized with additive 1.^{25,26} Here, the reduction in cell adhesion is not so obvious, which could be explained by the lower additive 1 to base material ratio of 5:95 compared to 10:90, as previously shown by Van Almen et al.²⁶ for HUVECs and 3T3 fibroblast cells cultured on drop-cast films up to 7 days. Furthermore, Mollet et al.²⁵ showed a reduction of cell adhesion for additive 1 to base material ratio of 30:70 for HK-2 cells on electrospun meshes, cultured for 14 h. Interestingly, additives 2 and 3 do reduce the cell adhesion clearly even though the absolute amount of PEG mixed in does not vary much: 1:1.2:1.2 for additive 1:2:3 (Table S7; calculation is provided in Supporting Information), suggesting that the length of the PEG chain and improved anchoring in the PCLdiUPy base polymer due to the additional alkyl spacer are of importance for non-cell-adhesive properties, whereas the different number of anchoring points between additives 2 and 3 does not appear to have an effect.

Quantification of Protein Adsorption Using QCM-D. The thickness of the polymer films on the QCM-D sensors was estimated by comparing the frequency shift of the empty sensors with that of the spin-coated sensors. The frequency shift has been converted to layer thickness using the Sauerbrey equation and a polymer density of 1145 kg/m^3 . For all mixtures, films of approximately 100 nm thick were obtained (Figure S3) showing that spin-coating indeed leads to reproducible, thin films.

QCM-D measurements were performed to quantify the amount of protein adsorbed under physiologically relevant

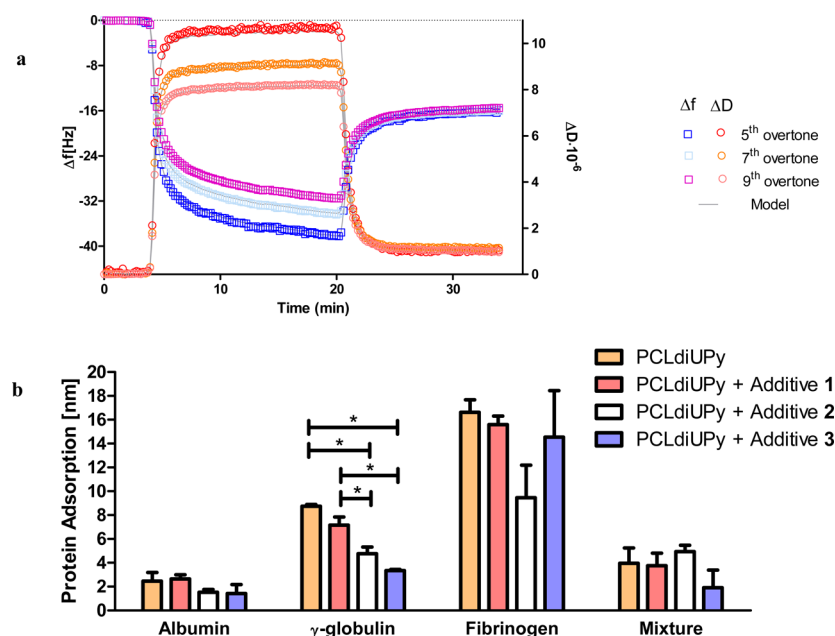


Figure 3. Protein adsorption as measured by QCM-D. (a) Example of frequency and dissipation changes as a function of time during the adsorption of albumin. For clarity, every tenth data point for the fifth, seventh, and ninth overtone is shown. (b) Overview of the adsorption of albumin (30 mg/mL), γ -globulin (10 mg/mL), fibrinogen (3 mg/mL), and a mixture of these three proteins under physiological conditions (37 °C) on spin-coated polymer films. Adsorption is represented as mean \pm SD ($N \geq 3$). * $P \leq 0.01$.

conditions. Representative data for one experiment, in which the adsorption of albumin is measured, is shown in Figure 3a. After equilibration with PBS at 37 °C, adsorption of mass can be observed upon introduction of a solution of 30 mg/mL albumin in PBS. Exposure of the PCLdiUPy-coated sensors to the albumin solution resulted in a frequency shift (Δf) for the fifth overtone of 42.6 ± 3.6 Hz. This frequency shift was accompanied by a dissipation shift (ΔD) of $(10.8 \pm 0.3) \times 10^{-6}$. The large $\Delta D/\Delta f$ ratio of 0.25 indicates the nonrigid coupling of mass to the sensor, which can be largely attributed to the viscosity of the albumin solution.²⁹ After rinsing with PBS, Δf decreases, and the overtones overlap. Furthermore, ΔD approaches 0 and the ratio $\Delta D/\Delta f \approx 5\%$. This indicates that the remaining adsorbed mass is more rigidly coupled to the sensor after rinsing.

Because of the large dissipation values, the Sauerbrey equation for rigid coupled mass is not valid, and the Voight–Voinova model was used.³⁰ In this study, one viscoelastic layer was used to model the protein adsorption and thus obtain parameters for the shear modulus, the shear viscosity, and the thickness (or mass) of the adsorbed protein layer. Furthermore, the bulk viscosity was allowed to vary. The protein density was set at 1250 kg/m^3 , which accounts for approximately 50% of surface coverage.¹⁴ Varying the protein density between 1000 kg/m^3 (density of water) and 1400 kg/m^3 (density of proteins) is known to have limited effect of the modeled mass and hence on the results obtained.³¹ Using this model, good fits to the data can be obtained (Figure 3a).

As expected, the viscosity of the albumin solution is similar for the different films (Table S2). The comparable values obtained for the Voigt mass while the sensor is immersed in the albumin solution and the Sauerbrey mass after rinsing with PBS further supports the hypothesis that the spread in overtones and large dissipation values are largely due to the viscosity of the albumin solution for the adsorption of albumin on pristine PCLdiUPy and indicate that hardly any albumin is removed

from the surface after rinsing. The Voigt mass has been converted to the thickness of the adsorbed protein layer using the protein density. For mixtures with additives 2 and 3 a trend can be observed toward less adsorption of albumin on the films, but the differences are not significant (Figure 3b). The protein layers are approximately 2 nm thick for all samples, which indicates the formation of a monolayer, consistent with results found previously for albumin.³² Therefore, the samples containing additive 2 or 3 are probably not fully covered by albumin.

Next, the adsorption of γ -globulin from a 10 mg/mL solution was studied as general model for globulins. The modeled bulk viscosity indicates that the solution is less viscous (Table S3). Similarly to the albumin adsorption, the Voigt mass is comparable to the Sauerbrey mass after rinsing with PBS. Furthermore, shear moduli indicate the formation of a solid layer. The layer thickness shows the same trend as the albumin adsorption. Again, hardly any reduction is observed for the sample containing additive 1. In contrast to the adsorption of albumin, a significant decrease in adsorption can be observed when the surfaces are PEGylated with additive 2 or 3 (Figure 3b). The mixture with additive 2 reduces the adsorption by 40%, and the mixture with additive 3 shows a reduction of 60% in adsorption compared to pristine PCLdiUPy. Values between 100 and 800 ng/cm^2 have been reported before for the adsorption of γ -globulin.³³

For the third protein in the Vroman series, fibrinogen, a concentration of 3 mg/mL was used. The viscosity of the solution is similar to the viscosity of the γ -globulin solution (Table S4). In this case, adsorption decreases with increasing molecular weight of the PEG, but the differences are not significant (Figure 3b). This is partially as a result of the large variation in adsorbed values measured using QCM-D (Table S4). The layer thickness of around 15 nm is lower than the long axis of fibrinogen of 47 nm, but twice the short axis of 5–7 nm.

A likely explanation is that the proteins adsorb not end-on but orientate sideways as suggested before for softer layers.³⁴

Although above results give insights into the adsorption of the individual components in blood plasma on biomaterials, *in vivo* the proteins are always mixtures. Therefore, all tested proteins were added in a single solution at the same concentrations as used above (albumin: 30 mg/mL; γ -globulin: 10 mg/mL; fibrinogen: 3 mg/mL) and introduced in the QCM-D. Even though the increased viscosity of the solution leads to large dissipation values, viscoelastic modeling allows for the separation of the contribution from the solvent and the adsorbed protein layer (Table S5). Here, a large discrepancy between the Voigt and the Sauerbrey mass after rinsing with PBS is observed, which might be a result of either soft, flexible protein layers or an effect of the shear stresses due to the more viscous solution. The decreased modeled viscosity for polymer films containing additive 3 shows that the model obtained for this sample needs to be interpreted with caution, but the trends match the values obtained for the Sauerbrey mass after rinsing with PBS.

The protein layers formed on the polymer films consisting of the pristine PCLdiUPy, the mixture with additive 1, and the mixture with additive 3 were slightly thicker than the layers formed from the solution of albumin, suggesting that mainly albumin adsorbs, which subsequently prevents the adsorption of the other proteins in these mixtures. For the sample with additive 2 the thickness of the protein layer is larger than the thickness of the albumin layer, suggesting that on this sample not only albumin but also the other proteins adsorb.

Experiments using optical waveguide light mode spectroscopy on block copolymers containing PEG have also shown that albumin can block the adsorption of other proteins when studied sequentially.³⁵ Although the hydrophilic UPyPEGs can reduce the adsorption of γ -globulin and fibrinogen, this effect appears to be canceled by the fast adsorption of albumin on these films.

Even though the reduction in protein adsorption is limited after mixing in 5 wt % of the UPyPEG additives, the adhesion of epithelial and endothelial cells is strongly impeded on films of polymer mixtures with additives 2 and 3. The results on cell adhesion are in accordance with a slight reduction in adsorption of γ -globulin on mixtures with additives 2 and 3 but do not match the adsorption of the other protein solutions studied here. Importantly, in previous studies, when a reduction in cell adhesion is observed on materials that also resist the adsorption of proteins, protein fouling is commonly measured prior to cell adhesion.^{2,6,9,11,12}

SUMMARY AND CONCLUSIONS

With these three additives, we have created a toolbox to tune non-cell-adhesive properties of our biomaterials in a modular fashion. Incorporation of PEG_{10K}diUPy and MeOPEG_{5K}diUPy clearly reduced cell adhesion and spreading compared to the pristine material. Using QCM-D in combination with viscoelastic modeling, and thereby separating the contribution of solvent viscosity and protein adsorption, we showed that we are able to quantify the adsorption of proteins on PCLdiUPy surfaces modified in a supramolecular fashion with UPyPEG. The more hydrophilic surfaces created by incorporation of PEG_{2K}diUPy, MeOPEG_{5K}UPy, and PEG_{10K}diUPy had a limited effect on protein adsorption, which shows that non-cell-adhesive behavior cannot per definition be correlated with a possible reduction in protein adsorption.

ASSOCIATED CONTENT

Supporting Information

The Supporting Information is available free of charge on the ACS Publications website at DOI: 10.1021/acs.langmuir.7b00467.

Root-mean-square roughness measurements, raw data and modeled parameters for the adsorption of albumin, γ -globulin, fibrinogen, and a mixture of the three, AFM height micrographs of spin-coated films, fluorescence microscopy image in grayscale of HK-2 and HUVECs, quantification of cell surface coverage, thickness of spin-coated polymer films as measured with QCM-D, and calculations of PEG amounts in mixtures with UPyPEG (PDF)

AUTHOR INFORMATION

Corresponding Author

*E-mail: p.y.w.dankers@tue.nl

ORCID

Patricia Y. W. Dankers: 0000-0002-8997-181X

Author Contributions

A.C.H.P. and B.D.I. contributed equally.

Notes

The authors declare no competing financial interest.

ACKNOWLEDGMENTS

The authors thank Moniek Schmitz for initial experiments on drop-casts of the mixtures and Olga Goor for the useful discussions on QCM-D measurements. This work was funded by the Ministry of Education, Culture and Science (Gravity program 024.001.035), The Netherlands Organisation for Scientific Research (NWO), the European Research Council (FP7/2007-2013) ERC Grant Agreement 308045, The Netherlands Institute for Regenerative Medicine, and ZonMW as part of the LSH 2Treat program (project number 436001003). This research forms part of the Project P1.03 PENT of the research program of the BioMedical Materials institute, cofunded by the Dutch Ministry of Economic Affairs.

REFERENCES

- (1) Wei, Q.; Becherer, T.; Angioletti-Uberti, S.; Dzubiella, J.; Wischke, C.; Neffe, A. T.; Lendlein, A.; Ballauff, M.; Haag, R. Protein Interactions with Polymer Coatings and Biomaterials. *Angew. Chem., Int. Ed.* **2014**, *53* (31), 8004–8031.
- (2) Ostuni, E.; Chapman, R. G.; Liang, M. N.; Meluleni, G.; Pier, G.; Ingber, D. E.; Whitesides, G. M. Self-Assembled Monolayers That Resist the Adsorption of Cells. *Langmuir* **2001**, *17* (7), 6336–6343.
- (3) Ostuni, E.; Chapman, R. G.; Holmlin, R. E.; Takayama, S.; Whitesides, G. M. A Survey of Structure-Property Relationships of Surfaces That Resist the Adsorption of Protein. *Langmuir* **2001**, *17* (18), 5605–5620.
- (4) Banerjee, I.; Pangule, R. C.; Kane, R. S. Antifouling Coatings: Recent Developments in the Design of Surfaces That Prevent Fouling by Proteins, Bacteria, and Marine Organisms. *Adv. Mater.* **2011**, *23* (6), 690–718.
- (5) Chen, S.; Li, L.; Zhao, C.; Zheng, J. Surface Hydration: Principles and Applications toward Low-Fouling/nonfouling Biomaterials. *Polymer* **2010**, *51* (23), 5283–5293.
- (6) Hucknall, A.; Rangarajan, S.; Chilkoti, A. In Pursuit of Zero: Polymer Brushes That Resist the Adsorption of Proteins. *Adv. Mater.* **2009**, *21* (23), 2441–2446.
- (7) Surman, F.; Riedel, T.; Bruns, M.; Kostina, N. Y.; Sedláková, Z.; Rodriguez-Emmenegger, C. Polymer Brushes Interfacing Blood as a

Route toward High Performance Blood Contacting Devices. *Macromol. Biosci.* **2015**, *15* (5), 636–646.

(8) Zhang, Z.; Zhang, M.; Chen, S.; Horbett, T. A.; Ratner, B. D.; Jiang, S. Blood Compatibility of Surfaces with Superlow Protein Adsorption. *Biomaterials* **2008**, *29* (32), 4285–4291.

(9) Harrison, R. H.; Steele, J. A. M.; Chapman, R.; Gormley, A. J.; Chow, L. W.; Mahat, M. M.; Podhorska, L.; Palgrave, R. G.; Payne, D. J.; Hettiaratchy, S. P.; et al. Modular and Versatile Spatial Functionalization of Tissue Engineering Scaffolds through Fiber-Initiated Controlled Radical Polymerization. *Adv. Funct. Mater.* **2015**, *25* (36), 5748–5757.

(10) Kostina, N. Y.; Pop-Georgievski, O.; Bachmann, M.; Neykova, N.; Bruns, M.; Michálek, J.; Bastmeyer, M.; Rodriguez-Emmenegger, C. Non-Fouling Biodegradable Poly(ϵ -Caprolactone) Nanofibers for Tissue Engineering. *Macromol. Biosci.* **2016**, *16* (1), 83–94.

(11) Sharma, S.; Johnson, R. W.; Desai, T. A. Evaluation of the Stability of Nonfouling Ultrathin Poly(Ethylene Glycol) Films for Silicon-Based Microdevices. *Langmuir* **2004**, *20* (2), 348–356.

(12) Chen, D.; Wu, M.; Li, B.; Ren, K.; Cheng, Z.; Ji, J.; Li, Y.; Sun, J. Layer-by-Layer-Assembled Healable Antifouling Films. *Adv. Mater.* **2015**, *27* (39), 5882–5888.

(13) Leonard, E. F.; Vroman, L. Is the Vroman Effect of Importance in the Interaction of Blood with Artificial Materials? *J. Biomater. Sci., Polym. Ed.* **1992**, *3* (1), 95–107.

(14) Höök, F.; Vörös, J.; Rodahl, M.; Kurrat, R.; Böni, P.; Ramsden, J.; Textor, M.; Spencer, N.; Tengvall, P.; Gold, J.; et al. A Comparative Study of Protein Adsorption on Titanium Oxide Surfaces Using in Situ Ellipsometry, Optical Waveguide Lightmode Spectroscopy, and Quartz Crystal Microbalance/dissipation. *Colloids Surf., B* **2002**, *24* (2), 155–170.

(15) Ferreira, G. N. M.; da-Silva, A.-C.; Tomé, B. Acoustic Wave Biosensors: Physical Models and Biological Applications of Quartz Crystal Microbalance. *Trends Biotechnol.* **2009**, *27* (12), 689–697.

(16) Cozzens, D.; Luk, A.; Ojha, U.; Ruths, M.; Faust, R. Surface Characterization and Protein Interactions of Segmented Polyisobutylene-Based Thermoplastic Polyurethanes. *Langmuir* **2011**, *27* (23), 14160–14168.

(17) Yang, R.; Gleason, K. K. Ultrathin Antifouling Coatings with Stable Surface Zwitterionic Functionality by Initiated Chemical Vapor Deposition (iCVD). *Langmuir* **2012**, *28* (33), 12266–12274.

(18) Dubois, J.; Gaudreault, C.; Vermette, P. Biofouling of Dextran-Derivative Layers Investigated by Quartz Crystal Microbalance. *Colloids Surf., B* **2009**, *71* (2), 293–299.

(19) Zhang, B.; Nagle, A. R.; Wallace, G. G.; Hanks, T. W.; Molino, P. J. Functionalised Inherently Conducting Polymers as Low Biofouling Materials. *Biofouling* **2015**, *31* (6), 493–502.

(20) Thalla, P. K.; Fadlallah, H.; Liberelle, B.; Lequoy, P.; De Crescenzo, G.; Merhi, Y.; Lerouge, S. Chondroitin Sulfate Coatings Display Low Platelet but High Endothelial Cell Adhesive Properties Favorable for Vascular Implants. *Biomacromolecules* **2014**, *15* (7), 2512–2520.

(21) Sijbesma, R. P.; Beijer, F. H.; Brunsveld, L.; Folmer, B. J.; Hirschberg, J. H.; Lange, R. F.; Lowe, J. K.; Meijer, E. W. Reversible Polymers Formed from Self-Complementary Monomers Using Quadruple Hydrogen Bonding. *Science* **1997**, *278* (5343), 1601–1604.

(22) Dankers, P. Y. W.; Harmsen, M. C.; Brouwer, L. A.; van Luyn, M. J. A.; Meijer, E. W. A Modular and Supramolecular Approach to Bioactive Scaffolds for Tissue Engineering. *Nat. Mater.* **2005**, *4* (7), 568–574.

(23) Wisse, E.; Spiering, A. J. H.; Dankers, P. Y. W.; Mezari, B.; Magusin, P. C. M. M.; Meijer, E. W. Multicomponent Supramolecular Thermoplastic Elastomer with Peptide-Modified Nanofibers. *J. Polym. Sci., Part A: Polym. Chem.* **2011**, *49* (8), 1764–1771.

(24) Dankers, P. Y. W.; Boomker, J. M.; Huizinga-van der Vlag, A.; Smedts, F. M. M.; Harmsen, M. C.; Van Luyn, M. J. A. The Use of Fibrous, Supramolecular Membranes and Human Tubular Cells for Renal Epithelial Tissue Engineering: Towards a Suitable Membrane for a Bioartificial Kidney. *Macromol. Biosci.* **2010**, *10* (11), 1345–1354.

(25) Mollet, B. B.; Comellas-Aragonès, M.; Spiering, A. J. H.; Söntjens, S. H. M.; Meijer, E. W.; Dankers, P. Y. W. A Modular Approach to Easily Processable Supramolecular Bilayered Scaffolds with Tailorable Properties. *J. Mater. Chem. B* **2014**, *2* (17), 2483.

(26) Van Almen, G. C.; Talacua, H.; Ippel, B. D.; Mollet, B. B.; Ramaekers, M.; Simonet, M.; Smits, A. I. P. M.; Bouten, C. V. C.; Kluin, J.; Dankers, P. Y. W. Development of Non-Cell Adhesive Vascular Grafts Using Supramolecular Building Blocks. *Macromol. Biosci.* **2016**, *16* (3), 350–362.

(27) Kieltyka, R. E.; Pape, A. C. H.; Albertazzi, L.; Nakano, Y.; Bastings, M. M. C.; Voets, I. K.; Dankers, P. Y. W.; Meijer, E. W. Mesoscale Modulation of Supramolecular Ureidopyrimidinone-Based Poly(ethylene Glycol) Transient Networks in Water. *J. Am. Chem. Soc.* **2013**, *135* (30), 11159–11164.

(28) Geiger, B.; Tokuyasu, K. T.; Dutton, A. H.; Singer, S. J. Vinculin, an Intracellular Protein Localized at Specialized Sites Where Microfilament Bundles Terminate at Cell Membranes. *Proc. Natl. Acad. Sci. U. S. A.* **1980**, *77* (7), 4127–4131.

(29) Reviakine, I.; Johannsmann, D.; Richter, R. P. Hearing What You Cannot See and Visualizing What You Hear. *Anal. Chem.* **2011**, *83* (23), 8838–8848.

(30) Voinova, M. V.; Rodahl, M.; Jonson, M.; Kasemo, B. Viscoelastic Acoustic Response of Layered Polymer Films at Fluid-Solid Interfaces: Continuum Mechanics Approach. *Phys. Scr.* **1999**, *59* (5), 391–396.

(31) Dutta, A. K.; Nayak, A.; Belfort, G. Viscoelastic Properties of Adsorbed and Cross-Linked Polypeptide and Protein Layers at a Solid-Liquid Interface. *J. Colloid Interface Sci.* **2008**, *324* (1–2), 55–60.

(32) Teichroeb, J. H.; Forrest, J. A.; Jones, L. W.; Chan, J.; Dalton, K. Quartz Crystal Microbalance Study of Protein Adsorption Kinetics on poly(2-Hydroxyethyl Methacrylate). *J. Colloid Interface Sci.* **2008**, *325* (1), 157–164.

(33) Lord, M. S.; Stenzel, M. H.; Simmons, A.; Milthorpe, B. K. The Effect of Charged Groups on Protein Interactions with poly(HEMA) Hydrogels. *Biomaterials* **2006**, *27* (4), 567–575.

(34) Doliška, A.; Ribitsch, V.; Stana Kleinschek, K.; Strnad, S. Viscoelastic Properties of Fibrinogen Adsorbed onto Poly(ethylene Terephthalate) Surfaces by QCM-D. *Carbohydr. Polym.* **2013**, *93* (1), 246–255.

(35) Leclercq, L.; Modena, E.; Vert, M. Adsorption of Proteins at Physiological Concentrations on Pegylated Surfaces and the Compatibilizing Role of Adsorbed Albumin with Respect to Other Proteins according to Optical Waveguide Lightmode Spectroscopy (OWLS). *J. Biomater. Sci., Polym. Ed.* **2013**, *24* (13), 1499–1518.